

## ***Ab initio* simulations of dense liquid deuterium: Comparison with gas-gun shock-wave experiments**

Stanimir A. Bonev, Burkhard Militzer, and Giulia Galli

*Lawrence Livermore National Laboratory, University of California, Livermore, California 94550, USA*

(Received 2 May 2003; revised manuscript received 21 October 2003; published 8 January 2004)

We present first-principles molecular-dynamics simulations of the equation of state of liquid deuterium up to eightfold compression and temperatures between 2000 and 20 000 K. We report significant technical improvements over previous density-functional calculations leading to excellent agreement with gas gun shock wave measurements, which have provided well established experimental data for the deuterium Hugoniot. The principal Hugoniot is further investigated by performing simulations with rigid deuterium molecules. We also compute the double-shock Hugoniot curve and compare calculated and measured reshock temperatures.

DOI: 10.1103/PhysRevB.69.014101

PACS number(s): 62.50.+p, 02.70.-c, 64.30.+t, 61.20.-p

### **I. INTRODUCTION**

Dense hydrogen has generated widespread interest for several decades and has been the focus of many research initiatives. Recently, several dynamic shock techniques have been used to study compressed fluid deuterium. Da Silva *et al.*<sup>1</sup> combined these techniques with a laser drive and probed the deuterium equation of state (EOS) up to pressures of 340 GPa. These measurements challenged the existing understanding of hot dense deuterium by showing a 50% higher compressibility than previously estimated. As a consequence, a series of follow-up experiments<sup>2-6</sup> and a large number of theoretical efforts have been initiated.<sup>7-12</sup> However, the controversy about the deuterium compressibility has not yet been settled. Recent shock measurements with magnetically driven flyer<sup>4,5</sup> showed a comparatively low compressibility, close to four times the initial density, in relatively good agreement with the Sesame model<sup>13</sup> and with path-integral Monte Carlo (PIMC) simulations.<sup>8</sup> Laser-driven shock experiments<sup>1-3</sup> predict instead up to sixfold compression and yield data consistent with a free-energy model proposed by Ross.<sup>14</sup> As a result of this discrepancy, considerable attention is now being paid to older gas gun shock wave experiments<sup>15,16</sup> that reached first-shock pressure up to 23 GPa. These measurements are well established and are used as a reference for the validation of new experimental techniques as well as a benchmark of theoretical predictions.

Among *ab initio* methods used to study hydrogen, only molecular dynamics simulations based on density-functional theory (DFT-MD) within a local-density approximation (LDA) and a generalized gradient approximation (GGA) have been applied below 50 GPa. In a previous study,<sup>7</sup> it was found that DFT-MD underestimates the shock pressures and temperatures by more than 30% compared with gas gun data. This has raised questions about the validity of LDA/GGA for the description of compressed hydrogen and its isotopes; in particular, it has been suggested that DFT at the level of a LDA underestimates the dissociation energy of D<sub>2</sub> in the compressed fluid,<sup>17</sup> thus leading to a stiff and “featureless” Hugoniot curve, and reshock temperatures much higher than those measured by Holmes *et al.*<sup>16</sup>

In this paper, we demonstrate that accurate DFT-MD

simulations actually yield an excellent agreement with gas gun measurements of pressure and temperature, and are consistent with recent independent calculations by Desjarlais.<sup>18</sup> The computed reshock temperatures are also in better agreement with experimental results than previously predicted.<sup>16,19</sup> The degree of molecular dissociation has a significant influence on the thermodynamic properties of the fluid and its precise determination requires very careful simulations. We consider the agreement with experiments obtained in our simulations as an indication that DFT within LDA/GGA can indeed be used to correctly predict properties of shocked deuterium. The computed principal Hugoniot flattens significantly above 23 GPa (and 4500 K) where stable molecules no longer exist. It eventually merges with the results previously reported<sup>7</sup> above 30 GPa, thus recovering the DFT prediction for a maximum compression ratio of 4.6. At higher densities, we find that molecular dissociation occurs rapidly, leading to a discontinuous or negative  $dP/dT|_V$ , which is consistent with the existence of a first-order liquid-liquid phase transition.

The rest of the paper is organized as follows. Section II describes the method used in the present study and Sec. III reports our results on the primary and double-shock deuterium Hugoniot. Sec. IV contains our conclusions.

### **II. COMPUTATIONAL METHOD**

Our *ab initio* MD simulations were carried out with the GP code,<sup>20</sup> using plane-wave basis sets, a  $\Gamma$ -point sampling of the Brillouin zone, and the Car-Parrinello (CP) method.<sup>21</sup> The use of CP dynamics, where the electronic and ionic degrees of freedom are propagated simultaneously, reduces systematic errors in the trajectories compared with Born-Oppenheimer MD. Depending on the density and temperature, we integrated the equations of motion with time steps between 0.4 and 2.5 a.u. (1 a.u. = 0.0249 fs) and a corresponding fictitious electronic mass ranging from 6 to 120 a.u.

We used a norm-conserving pseudopotential of the Troullier Martins-type<sup>22</sup> with a 60 Ry plane-wave cutoff, which leads to an excellent description of the zero-pressure fluid (see Sec. III). In the case of hydrogen, the accuracy and transferability of norm-conserving pseudopotentials (PP) can

be easily and more straightforwardly insured than those of ultrasoft PP, used, for example, in Ref. 7 to describe the low-pressure Hugoniot of deuterium. We note that in the ultrasoft PP scheme, norm conservation is initially not imposed on the pseudowave function, thus allowing one to use a lower energy cutoff. The norm conservation is then restored by adding augmentation wave functions in the core region. In the case of hydrogen, where there is no distinction between core and valence electrons, the transferability of ultrasoft PP to correctly describe the bonding properties over a large density range may be difficult to control. In addition, the calculation of the nonlocal part of the PP energy requires special care when using ultrasoft PP, especially if carried out in real space where issues of nontranslational invariance of the Hamiltonian introduced by the nonlocal PP operator need to be addressed. Therefore, we believe that the use of norm-conserving pseudopotentials may be a significant reason for the technical improvement found in our paper over Ref. 7 (see Sec. III).

We also note that the energy cutoffs ( $E_{\text{cut}}$ ) used to represent the Kohn-Sham orbitals with ultrasoft and norm-conserving PP are not directly comparable. The  $E_{\text{cut}}$  used in the case of norm-conserving PP is appropriate to expand the norm-conserving atomic wave functions, but a cutoff four times as large ( $E_{\text{cut}}^p$ ) is used for the expansion of the charge density and potential. In the case of ultrasoft PP,  $E_{\text{cut}}$  is appropriate to expand only the tail of the atomic wave functions (i.e., a softer, non-norm-conserving approximation of the wave functions, which matches only the tail of the physical wave functions); this cutoff is usually much smaller than four times the cutoff used to expand the charge density once norm conservation of the wave functions is restored. Therefore, in order to meaningfully compare the accuracy of ultrasoft and norm-conserving PP, one needs to compare  $E_{\text{cut}}^p$ , and not  $E_{\text{cut}}$ , used in the two cases.

In all of our simulations, the exchange-correlation energy was calculated within the Perdew-Burke-Ernzerhof<sup>23</sup> GGA using a zero-temperature energy functional. Recently, Surh *et al.*<sup>24</sup> calculated the Hugoniot of aluminum using finite-temperature exchange-correlation functionals, but found only a shift in the density, noticeable above  $3 \times 10^5$  K, and nearly unchanged pressure of the Hugoniot points with respect to using a zero-temperature functional. Therefore, for the temperatures of interest here—all except one below  $10^4$  K, the use of zero-temperature exchange-correlation for the Hugoniot calculations seems to be well justified. For higher temperatures or/and different quantities, other approaches may become preferable.

In our study, we performed a series of constant-volume simulations with supercells containing 128 atoms at densities and temperatures targeted to bracket the primary and reshock Hugoniot curves. The initial fluid configuration at each density was prepared by classical MD (Ref. 25) simulation of a fluid with rigid D<sub>2</sub> molecules. The *ab initio* DFT-MD simulations were then carried out for at least 1 ps and until a good convergence of the pressure to a constant average value was attained and maintained for not less than 0.5 ps. For the lower densities and temperatures, this required simulation times of about 3ps, and in the case of  $\rho = 0.171 \text{ g cm}^{-3}$  and

$T = 20 \text{ K}$ , we had to first heat and then quench the system in order to obtain the zero-pressure result. To study size effects (including the sufficiency of the  $\mathbf{k}$ -point sampling), we performed simulations with supercells containing 250 atoms at  $\rho = 0.587 \text{ g cm}^{-3}$  ( $4000 \text{ K} < T < 5500 \text{ K}$ ) and  $\rho = 0.732 \text{ g cm}^{-3}$  ( $T = 5000 \text{ K}$ )—conditions over which the fluid loses its molecular character. We found only a small shift in the pressure relative to the 128 atom supercell simulations, namely a drop of 0.3 GPa in the molecular fluid, and an increase of 0.6 GPa in the dissociating regime.

We also repeated some of our simulations using the gradient corrected local spin density approximation and checked for possible spin effects (at  $0.679 \text{ g cm}^{-3}$  and 5000 K); this again resulted in only negligible changes ( $-0.3 \text{ GPa}$  and  $+0.02 \text{ eV}$ ) in the computed values of the pressure and energy. The reason for this is that in the dense fluid (whether molecular or dissociating) all orbitals are doubly occupied in a paramagnetic state, contrary to the case of an isolated molecule, where separating the atoms leads to an antiferromagnetic arrangement.

### III. RESULTS

We first discuss our results for the equation of state of deuterium and the primary Hugoniot (Sec. III A); we then compare our computed double-shock Hugoniot points with recent gas gun experiments (Sec. III B).

#### A. Primary Hugoniot

EOS values for the calculation of the primary Hugoniot are given in Table I. For each of the selected densities, the data are used to determine accurately the pressure ( $P$ ) and temperature ( $T$ ) that satisfy the Hugoniot equation,

$$E - E_0 = \frac{1}{2}(P + P_0)(1/\rho - 1/\rho_0), \quad (1)$$

where  $\rho_0 = 0.171 \text{ g cm}^{-3}$  is the initial density of liquid deuterium at 20 K,  $P_0 \approx 0$ , and  $E_0 = -15.87 \text{ eV}$  is the computed energy per atom at these conditions. The results are compared with gas gun experiments and previous DFT data in Fig. 1; the agreement with measured pressure and temperature is excellent. We believe that this improvement is due to technical differences between our *ab initio* simulations, using the CP algorithm and norm-conserving pseudopotentials, and those reported in Ref. 7, which were obtained with Born-Oppenheimer MD and ultrasoft pseudopotentials. In our calculations for  $\rho = 0.587 \text{ g cm}^{-3}$ , the fluid remains molecular up to about 4500 K. At higher temperatures, as the simulation progresses (keeping  $\rho = 0.587 \text{ g cm}^{-3}$  and  $T$  constant), the onset of dissociation is accompanied by a decrease in the pressure. These results do not appear to depend strongly on the supercell size at this density; however they are sensitive to the choice of integration time step and to the resulting optimization of the wave functions in the CP algorithm, and extreme care has been taken to obtain converged results. As the fluid enters a regime where stable molecules do not exist, the Hugoniot flattens and eventually merges with the curve of Ref. 7.

TABLE I. Pressure and internal energy per atom of D<sub>2</sub> fluid as a function of density and temperature from DFT-MD simulations. Uncertainties in the last digit are given in parentheses and are related to statistical averages during the simulations.

$r_s$	$\rho$ (g cm <sup>-3</sup> )	$T$ (K)	$P$ (GPa)	$E$ (eV)
3.167	0.171	20	0.04	-15.87
		2200 (20)	13.0 (2)	-15.38 (1)
2.20	0.509	2820 (20)	13.6 (2)	-15.28 (1)
		3500 (30)	15.3 (3)	-15.14 (1)
		3000 (25)	15.9 (3)	-15.22 (1)
2.15	0.546	3800 (30)	17.6 (2)	-15.05 (2)
		4500 (50)	19.0 (4)	-14.89 (3)
		3775 (40)	20.4 (4)	-15.00 (3)
		4000 (35)	21.2 (4)	-14.98 (1)
2.10	0.587	4530 (35)	22.8 (5)	-14.87 (2)
		5000 (40)	23.2 (7)	-14.74 (7)
		5500 (30)	23.3 (6)	-14.60 (5)
2.00	0.679	4490 (40)	25.5 (10)	-14.72 (7)
		4985 (45)	26.7 (7)	-14.61 (7)
		4980 (40)	29.0 (10)	-14.53 (7)
1.95	0.732	5970 (45)	30.1 (11)	-14.31 (6)
		6980 (30)	32.9 (6)	-14.13 (8)
		4985 (40)	32.5 (10)	-14.47 (6)
1.91	0.779	6975 (35)	37.7 (11)	-14.11 (7)
		9965 (40)	42.8 (10)	-13.64 (8)
		19860 (165)	78.2 (15)	-12.25 (22)

In Fig. 2, we show the pressure as a function of temperature for three different densities. At  $\rho = 0.546$  g cm<sup>-3</sup>, the molecules remain intact over the simulation times and the given temperature range, and  $P(T)$  is almost linear. At the higher density, the slope of  $P(T)$  changes as the molecules start to dissociate. We see no indication of discontinuity in  $P(T)$ , meaning that the transition is gradual—an argument

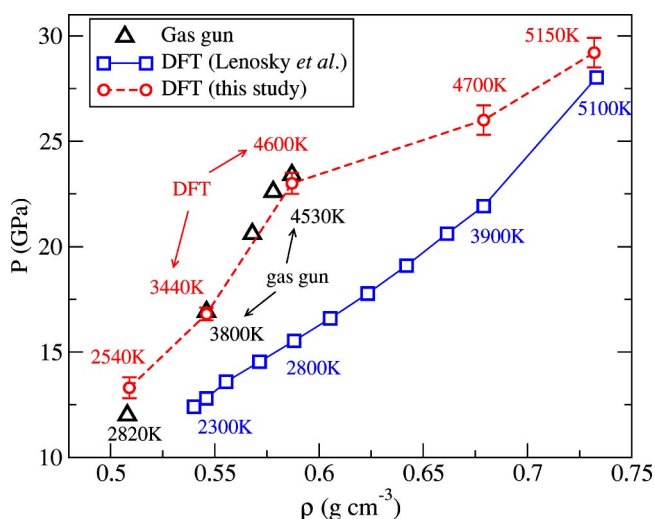


FIG. 1. Low-pressure part of the deuterium Hugoniot—comparison with gas gun measurements (Ref. 16) and previous DFT results (Ref. 7). Experimental uncertainties are within the size of the symbols.

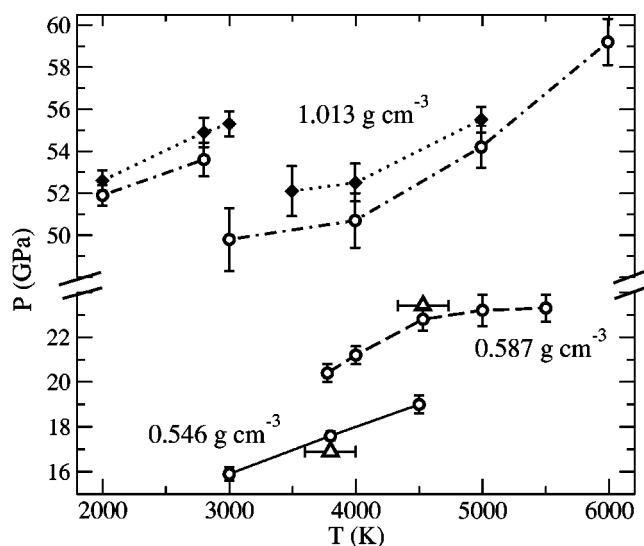


FIG. 2. Pressure vs temperature at selected densities corresponding to  $r_s = 2.15, 2.10,$  and  $1.75$ . Circles indicate calculated values with 128 atoms, diamonds are calculations with 256 atoms, triangles are gas gun measurements (Ref. 16) and the lines connecting the points are only guides to the eye. The size effects for  $0.587$  and  $0.546$  g cm<sup>-3</sup> are insignificant and are not shown.

also supported by the apparent lack of size effects, which would be present in the case of long correlation lengths close to a first-order phase transition. However, at  $\rho = 1.013$  g cm<sup>-3</sup>, there is a large drop in pressure when heating from 2800 to 3000 K, suggesting the existence of a first-order liquid-liquid phase transition in this  $P$ - $T$  region. To check sensitivity to size effects, we have performed calculations with 256-atom cells. The results, plotted in Fig. 2, show that the computed pressures increase consistently by about 1.5 GPa and the magnitude of the drop in  $P$  remains almost unchanged, but the transition temperature is shifted slightly upward as expected. We have observed such a sharp drop in the pressure also at lower density, namely, at  $\rho = 0.858$  g cm<sup>-3</sup> between 3000 and 4000 K. These observations are consistent with the results of other authors<sup>26</sup> who have reported a negative  $dP/dT|_V$  slope, and in particular with the very recently proposed<sup>27</sup> transition at 1500 K and 125 GPa. We note that there are numerous predictions of a plasma phase transition in dense liquid hydrogen in the literature,<sup>28</sup> including some on the principal Hugoniot.<sup>29</sup> Our results support the view that the shocked fluid dissociates gradually on the Hugoniot and that there is a critical point below 4500 K at higher densities.

The compressibility of deuterium observed in shock wave experiments is often explained in terms of molecular dissociation. In order to elucidate the differences between dissociating and purely molecular hydrogen, we performed DFT-MD simulations where we prevented dissociation by constraining the molecular bond lengths to 0.77 Å.<sup>30</sup> We performed the usual CP-MD, with the only exception that the bond lengths were now artificially kept constant using the SHAKE algorithm.<sup>31</sup> In order to mimic vibrating (harmonic) molecules, we have added  $k_B T$  to the energy of each D<sub>2</sub> pair obtained in the DFT simulations. The Hugoniot points com-

TABLE II. Principal Hugoniot densities, pressures, and temperatures computed with and without constrained molecular dissociation. Statistical uncertainties to the last digit are given in parentheses.

$\rho$ ( $\text{g cm}^{-3}$ )	Unconstrained MD		Constrained MD	
	$P$ (GPa)	$T$ (K)	$P$ (GPa)	$T$ (K)
0.509	13.3 (5)	2540 (50)		
0.546	16.8 (4)	3440 (100)		
0.587	23.0 (5)	4600 (150)	21.8 (5)	4400 (150)
0.679	26.0 (7)	4700 (200)	33.5 (15)	7500 (700)
0.732	29.2 (7)	5150 (200)		
0.779	39.5 (15)	7770 (300)		
0.779	62.7 (30)	15600 (800)	63 (4)	4500 (1000)

puted in this way are given in Table II together with the nonconstrained MD data, and they are plotted in Fig. 3 along with other theoretical and experimental results. As expected, restricting the dissociation does not vary the thermodynamic properties in any relevant way in the region where the unconstrained fluid is mostly molecular. However it leads to more repulsive interactions compared to the dissociating fluid and increases the pressure at intermediate densities and temperatures. In Fig. 3, we have also shown the results of the cusp-condition constraints approximation<sup>32</sup> (CCA), where proton-proton correlations beyond the core repulsive region are ignored. The deviations from the CCA reflect the importance of the longer-range interactions among the nuclei. Thus, the constrained MD calculations presented here and the CCA describe the two extremes of pure molecular and of pure atomic hydrogen, respectively, valid in the low- ( $P < 23$  GPa) and the high- ( $P > 200$  GPa, see Ref. 32 for details) pressure limits.

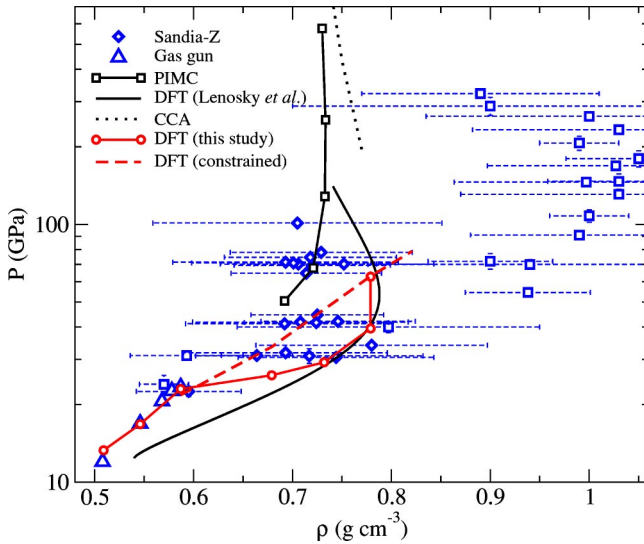


FIG. 3. Deuterium Hugoniot calculated with and without constrained molecular dissociation (see text)—compared to experimental data [NOVA (Refs. 1,2), Sandia-Z (Refs. 4,5), and gas gun (Ref. 16)], and to previous theoretical results: PIMC (Ref. 8), DFT (Ref. 7), and CCA (Ref. 32). For a meaningful comparison, the actual shock densities from the Sandia measurements have been rescaled here by 1.024, as the initial sample density in these experiments is  $0.167 \text{ g cm}^{-3}$ .

We note that at pressures above 100 GPa, the agreement between DFT/GGA and PIMC (Ref. 8) is fairly good, although a difference in the maximum compression ratio is observed: 4.6 in DFT compared to 4.3 in PIMC. This difference can come both from the different treatment of correlation in DFT and PIMC and from numerical approximations.<sup>33</sup> In general, PIMC predicts higher pressures and a lower degree of dissociation.

## B. Double-shock Hugoniot

Next, we turn our attention to the double-shock Hugoniot. Direct temperature measurements of the reshocked deuterium were reported in Ref. 16. They are an important constraint on the parameters of approximate free-energy models. For example, adjustments in the Ross model<sup>14</sup> to fit the reshock temperatures led to predict a high compressibility in agreement with the laser-driven experiments, while the RRY model<sup>19</sup> predicts a lower compressibility and reshock temperatures higher than the experimental values by as much as 2000 K.

We compare our results here with the five reshock measurements reported in Ref. 16. In this experiment, reshock states were generated by reflecting the primary shock wave off a back window material. Such a reflection also generates a shock wave in the back window, the principal Hugoniot of which gives the resulting thermodynamic conditions there. The Hugoniot curves of the window materials used in the experiment,  $\text{Al}_2\text{O}_3$  and  $\text{LiF}$ , are well characterized.<sup>34</sup> Furthermore, to derive the deuterium reshock states (for details see Ref. 10) we make use of impedance match, i.e., the pressure as well as the particle velocity (mass velocity behind the shock front) are considered continuous across the deuterium-window interface. A second necessary condition follows from Eq. (1) relating the primary shock state  $(E_1, \rho_1, P_1)$  to the reshock state  $(E_2, \rho_2, P_2)$ .

Using the DFT-EOS for the densities 0.86, 1.0, and  $1.0 \text{ g cm}^{-3}$ , we have determined the secondary shock temperatures and densities for the set of five gas gun primary shock states. The statistical uncertainty in the EOS is propagated in addition. The resulting primary and secondary shock temperatures are in good overall agreement with experiment, as shown in Fig. 4. DFT slightly underestimates the reshock temperature for low densities and overestimates it for high densities (by up to 1000 K). A more careful determination of

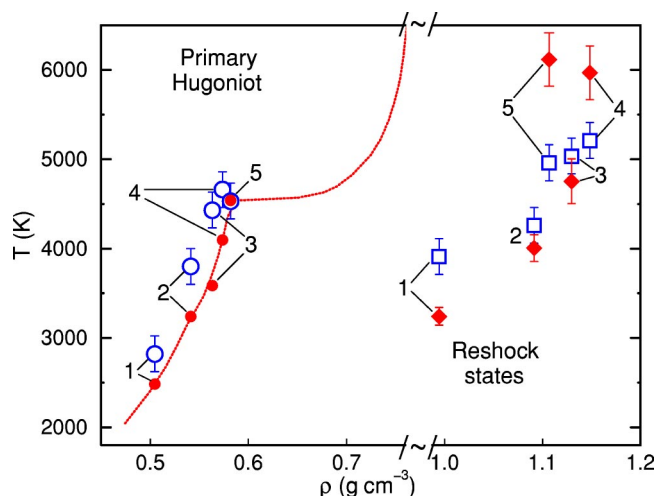


FIG. 4. First- and second-shock temperatures are shown as a function of density for five measurements (Ref. 16) (open symbols). Corresponding primary and secondary shock states are marked with the same label: 1–4 indicate measurements with a  $\text{Al}_2\text{O}_3$  back window and label 5 is for LiF as window material. Solid symbols are calculated values. The reshock densities were not measured and the computed values have been used instead.

the lowest reshock temperatures may require more simulations close to the liquid-liquid phase transition, where large fluctuations, long correlation lengths, and size effects become significant, and therefore it presents a formidable computational task. Such analysis goes beyond the scope of this paper and will be subject of future work.

#### IV. CONCLUSION

In summary, we have presented accurate EOS calculations of dense liquid deuterium using *ab initio* MD using DFT within the GGA. Significant technical improvements have led to excellent agreement with the gas gun measurements of pressure and temperature on the principal Hugoniot. Overall, our findings are consistent with the recent independent calculations by Desjarlais;<sup>18</sup> however we have focused on a comparison with gas gun measurements where the shape of the primary and reshocked Hugoniot curves have been examined in detail and related to the onset of molecular disso-

ciation. The maximum compression ratio found here, 4.6, is in agreement with that found in previous DFT calculations—4.6 in Ref. 7 and 4.5 in Ref. 18. Our results are also in qualitative accord with those of PIMC calculations where the maximum compression is 4.3. The remaining differences between the current DFT and PIMC descriptions could either come from different treatments of the exchange and correlation energies in the two approaches or from size effects and/or approximations of nodal surfaces in PIMC.

We have also calculated the double-shock Hugoniot, which yields relatively good agreement with measured reshock temperatures. Our DFT results predict that the double-shocked fluid may go through a first-order liquid-liquid phase transition. Theoretically, the existence and understanding of this phase transition remains an open question which may require investigations using *ab initio* methods beyond DFT/GGA. We note that PIMC calculations using free particle nodes by Magro *et al.*<sup>35</sup> predicted a first-order plasma phase transition (PPT) in dense liquid deuterium and indicated a negative  $dP/dT$  slope at a density of  $r_s = 1.86$  between 6000 and 8000 K. Subsequent PIMC simulations using a more accurate nodal surface<sup>36</sup> gave a different EOS at lower temperature and did not show a negative  $dP/dT$  slope at a density of  $r_s = 1.86$ . There are two possible interpretation for those findings—either the PPT disappears altogether when using variational nodes, or alternatively, it only shifts, e.g., to lower temperatures that cannot be accessed using PIMC at present. Both scenarios are possible. Experimentally, one could determine the principal Hugoniot above 23 GPa with higher accuracy than in Refs. 4,5 and verify if the proposed flattening is observed. Alternatively, one could look for the transition in reshock experimental states below 60 GPa.

#### ACKNOWLEDGMENTS

We thank M. Ross and G. Collins for stimulating this research project, D. Hicks for providing us with Hugoniot curves for the back plate materials, E. Schwegler for technical assistance, and N. Holmes and N. Ashcroft for useful discussions. This work was performed under the auspices of the U.S. Department of Energy at the University of California/LLNL under Contract No. W-7405-Eng-48.

<sup>1</sup>I.B. Da Silva *et al.*, Phys. Rev. Lett. **78**, 783 (1997).

<sup>2</sup>G.W. Collins, L.B.D. Silva, P. Celliers, D.M. Gold, M.E. Foord, R.J. Wallace, A. Ng, S.V. Weber, K.S. Budil, and R. Cauble, Science **281**, 1178 (1998).

<sup>3</sup>A. Mostovych, Y. Chan, T. Lehecha, A. Schmitt, and J. Sethian, Phys. Rev. Lett. **85**, 3870 (2000).

<sup>4</sup>M.D. Knudson, D.L. Hanson, J.E. Bailey, C.A. Hall, J.R. Asay, and W.W. Anderson, Phys. Rev. Lett. **87**, 225501 (2001).

<sup>5</sup>M.D. Knudson, D.L. Hanson, J.E. Bailey, C.A. Hall, and J.R. Asay, Phys. Rev. Lett. **90**, 035505 (2003).

<sup>6</sup>S.I. Belov *et al.*, JETP Lett. **76**, 433 (2002).

<sup>7</sup>T.J. Lenosky, S.R. Bickham, J.D. Kress, and L.A. Collins, Phys.

Rev. B **61**, 1 (2000).

<sup>8</sup>B. Militzer and D.M. Ceperley, Phys. Rev. Lett. **85**, 1890 (2000).

<sup>9</sup>G. Galli, R. Hood, A. Hazi, and F. Gygi, Phys. Rev. B **61**, 909 (2000).

<sup>10</sup>B. Militzer, D.M. Ceperley, J.D. Kress, J.D. Johnson, L.A. Collins, and S. Mazevet, Phys. Rev. Lett. **87**, 275502 (2001).

<sup>11</sup>F. Gygi and G. Galli, Phys. Rev. B **65**, 220102 (2002).

<sup>12</sup>M.W.C. Dharma-wardana and F. Perrot, Phys. Rev. B **66**, 014110 (2002).

<sup>13</sup>G. I. Kerley, in *Molecular Based Study of Fluids*, edited by J. M. Haili and G. A. Mansoori (ACS, Washington DC, 1983), p. 107.

<sup>14</sup>M. Ross, Phys. Rev. B **58**, 669 (1998).

- <sup>15</sup>W.J. Nellis, M. Ross, A.C. Mitchell, M. van Thiel, D.A. Young, F.H. Ree, and R.J. Trainor, *Phys. Rev. A* **27**, 608 (1983).
- <sup>16</sup>N.C. Holmes, M. Ross, and W.J. Nellis, *Phys. Rev. B* **52**, 15 835 (1995).
- <sup>17</sup>M. Ross and L.H. Yang, *Phys. Rev. B* **64**, 174102 (2001).
- <sup>18</sup>M.P. Desjarlais, *Phys. Rev. B* **68**, 064204 (2003).
- <sup>19</sup>M. Ross, F.H. Ree, and D.A. Young, *J. Chem. Phys.* **79**, 1487 (1983).
- <sup>20</sup>F. Gygi, Computer code GP 1.20.0 (Lawrence Livermore National Laboratory, California, 2003).
- <sup>21</sup>R. Car and M. Parrinello, *Phys. Rev. Lett.* **55**, 2471 (1985).
- <sup>22</sup>N. Troullier and J.L. Martins, *Phys. Rev. B* **43**, 1993 (1991).
- <sup>23</sup>J.P. Perdew, K. Burke, and M. Ernzerhof, *Phys. Rev. Lett.* **77**, 3865 (1996).
- <sup>24</sup>M.P. Surh, T.W. Barbee III, and L.H. Yang, *Phys. Rev. Lett.* **5958**, 064204 (2001).
- <sup>25</sup>Classical MD simulations were performed using the TINKER software (URL <http://dasher.wustl.edu/tinker>).
- <sup>26</sup>S. Bagnier, P. Blottiau, and J. Cl  rouin, *Phys. Rev. E* **63**, 015301 (2000).
- <sup>27</sup>S. Scandolo, *PNAS* **100**, 3051 (2003).
- <sup>28</sup>D. Beule, W. Ebeling, and A. F  rster, *Phys. Rev. B* **59**, 14 177 (1999), and reference therein.
- <sup>29</sup>D. Saumon and G. Chabrier, *Phys. Rev. A* **46**, 2084 (1992).
- <sup>30</sup>The equilibrium bond length in the gas phase.
- <sup>31</sup>S.I. Ryckaert, G. Ciccotti, and H.J.C. Berendsen, *J. Comput. Phys.* **23**, 327 (1977).
- <sup>32</sup>K. Nagao, S.A. Bonev, and N.W. Ashcroft, *Phys. Rev. B* **64**, 224111 (2001).
- <sup>33</sup>PIMC computations with 32 atom supercells yield  $47 \pm 5$  GPa at 10 000 K and  $0.67 \text{ g cm}^{-3}$ . At these conditions, DFT gives  $33.5 \pm 1.5$  and  $36.3 \pm 1.5$  GPa for 32 and 128 atom cells, respectively. Size effects originating from insufficient  $\mathbf{k}$ -point sampling may have opposite sign in PIMC and DFT-MD.
- <sup>34</sup>We use the following linear fits relating the shock and particle speeds (in km/s) in the back window materials— $\text{Al}_2\text{O}_3$ :  $u_s = (0.957u_p + 8.74)$  and  $\text{LiF}$ :  $u_s = (1.31u_p + 5.18)$ .
- <sup>35</sup>W.R. Magro, D.M. Ceperley, C. Pierleoni, and B. Bernu, *Phys. Rev. Lett.* **76**, 1240 (1996).
- <sup>36</sup>B. Militzer and E.L. Pollock, *Phys. Rev. E* **61**, 3470 (2000).